PHYSICAL REVIEW A **92**, 052708 (2015)

Angle-differential observation of plasmon electrons in the double-differential cross-section spectra of fast-ion-induced electron ejection from C_{60}

A. H. Kelkar,[1,2] L. Gulyás,[3] and Lokesh C. Tribedi[1,*]
[1]*Tata Institute of Fundamental Research, 1 Homi Bhabha Road, Colaba, Mumbai 400005, India*
[2]*Indian Institute of Technology Kanpur, Kanpur 208016, India*
[3]*Institute of Nuclear Research of the Hungarian Academy of Sciences (ATOMKI), H-4001 Debrecen, Hungary*
(Received 16 April 2015; published 18 November 2015)

We report on the measurement of double-differential distribution of soft electron emission from C_{60} fullerene, induced by a fast-moving Coulomb field of 76 MeV energy bare fluorine ions. A broad "plasmon-electron" peak, riding on the Coulomb-ionization continuum, is observed due to the deexcitation of the giant dipole plasmon resonance state in C_{60}. The angular distribution of the plasmon electrons goes through a dip around 90°, which is contrary to that observed in ion-atom collisions measured *in situ*, indicating the alignment of the induced dipole moment along the projectile beam direction. A model based on the photoelectron angular distribution which is modified due to the ion-induced postcollisional interaction provides an excellent agreement with the observed asymmetric distribution. The distribution smoothly changes from a dip at 90° to a peak with the variation of ejected electron energy indicating transition from a collective plasmon behavior of the whole system to a single ion-atom interaction. The single-differential cross section was also derived, which preserves the signature of the collective excitation.

DOI: 10.1103/PhysRevA.92.052708 PACS number(s): 34.50.Fa, 36.40.Gk, 61.48.−c

I. INTRODUCTION

Recently, complex allotropes of carbon, such as fullerenes and nanotubes, as well as large organic molecules of biological importance, such as RNA and DNA bases, and astrophysical relevance, such as linear and cyclic carbon chains, have been at the focus of atomic-collision research. The interest in these systems arises since one needs to understand the influence of the many-body nature on ionization and charge-transfer processes. In a recent study, it was shown that uracil, which is a ring-shaped organic molecule, has a dramatically large cross section for electron emission, particularly at forward angles, and this behavior cannot be explained in the realm of conventional ion-atom collision models [1]. Similarly, the collective excitation in polycyclic aromatic hydrocarbon (PAH) molecules [2], found in the interstellar medium, also influences their interaction with charged particles and photons. Although there has been major progress in understanding the structural complexity of these organic molecules, there is still a lack of a sophisticated theoretical framework to explore their collision dynamics with heavy-charged particles. The collision dynamics of large and complex organic molecules is mainly governed by many-electron processes. This can be better studied by forging a synergy with large-ordered molecules, such as fullerenes, which are known to show strong many-body correlations.

Carbon fullerenes, with a diameter of about one nanometer, have a highly symmetric hollow core held firmly by a delocalized cloud of a large number of valence electrons. The structure and properties of fullerenes have been probed extensively with photons, electrons, and heavy ions. For example, the collective oscillations of these delocalized σ and π valence electrons in C_{60} fullerene give rise to a Mie-type surface plasmon resonance [3], which is also known as giant dipole plasmon resonance (GDPR). This GDPR in fullerenes [4–14] is, to some extent, analogous to the well-known nuclear giant dipole resonance [15], plasmon excitation in solids and metallic clusters [16], as well as shape resonances in large atoms (e.g., Xe) [17]. This collective behavior of electrons in solids is known to give rise to dynamic screening and a wake of electron-density fluctuations [18,19]. The influence of the solid-state effect on different collision processes, such as radiative electron capture [20–22], resonant coherent excitation [23,24], and convoy electron production, is already known. The influence of the GDPR on electron capture by fast highly charged ions from a free fullerene molecule has been studied using an x-ray technique [25]. The effect of this resonance on the ionization and fragmentation of C_{60} in collisions with photons and heavy ions was also reported earlier [6,26–31].

The heavy-ion collisions experiments [30,31] revealed a linear dependence of the total ionization cross section of fullerene on the projectile charge state (q), in contrast to the q^2 dependence observed in ion-atom collisions. The linear behavior in the case of the C_{60} molecule was explained in terms of a GDPR excitation [26,31] model. As explained in the earlier literature [14,32,33], the delocalized valence electrons in fullerenes are highly polarizable. The collective excitation of this polarizable electron cloud in fullerene is termed as plasmon excitation, in analogy with the collective response of free electrons in solids in the presence of an external electric field. It is known that such plasmons can be excited by swift charged particles or photons through their electromagnetic interactions with the delocalized electrons in the fullerene or metal clusters. It was suggested that the GDPR has a profound influence on the energy loss of the projectile. However, most of these studies were focused on measuring the GDPR contribution on the recoil-ion yields, whereas the electron-spectroscopy-based measurements using a free C_{60} molecule as the target are rather limited [9,34–37]. This lack of experimental investigations on electron spectroscopy of C_{60} can be, in part, attributed to the difficulties in detecting low-energy

*lokesh@tifr.res.in

electrons. In addition, the ejected electron spectrum is largely dominated by the single-particle Coulomb-ionization mechanism, where the cross section falls over several orders of magnitude in the emitted electron energy range, i.e., typically over 1–300 eV. This makes the observation of the secondary features in the electron spectrum even more challenging, which has already been demonstrated in the recent series of the study of the Young-type electron interference effect in ionization of H_2 [38,39] in heavy-ion impact. Nevertheless, the direct electron emission being the fastest mode of the deexcitation of the collective state GDPR [16] makes this study even more interesting. Furthermore, a direct observation of such GDPR electron peak in the double-differential cross-section (DDCS) spectrum will provide a more stringent test of the plasmon excitation models than the single-differential or the total cross sections. Projectile ions with high charge state and high velocity ($v_p \geqslant 10$ a.u.) are suitable choices for this investigation since the cross section of the GDPR excitation has been predicted [26] to be almost independent of projectile energy in the present velocity range, but increases linearly with q [26,31]. Thus, a fast highly charged projectile ion can efficiently transfer the energy required for the excitation of the plasmon resonance in C_{60} at an adiabatic distance ($b_0 = \gamma h v/2\pi E$ [26]) which is outside the C_{60} cage radius (r $\sim$ 5 Å) including the electron cloud extension. In the present experiment, this adiabatic distance is $\sim$ 9 Å. It is worth mentioning that the electron transfer probability is much smaller than the ionization probability in this velocity range ($v_p \gg v_e$, with v_e being the orbital velocity of the outer-shell electrons of a carbon atom which is about 1 a.u.), since the capture cross section varies as v_p^{-12}.

In this article, we present the energy (ϵ_e) and angular (Ω_e) distributions of the DDCS, i.e., $d^2\sigma/d\epsilon_e d\Omega_e$, in the case of the C_{60} target in collisions with the fast ($v \sim 12.7$ a.u.) bare F ions. While the DDCS spectrum provides a direct evidence of plasmon excitation in C_{60}, the angular distributions of low-energy electrons provide useful information about the nature of collective oscillation, i.e., whether it is a dipole- or quadrupole-type resonance, and about the alignment of the dipole moment with respect to the beam axis, etc.

II. EXPERIMENTAL DETAILS AND MEASUREMENT

A beam of 76 MeV F^{9+} ions was obtained from the tandem Pelletron accelerator at TIFR, Mumbai. The ions were made to collide with the 99% pure C_{60} vapor target in a high vacuum scattering chamber. Energy and angular (30° to 150°) distribution spectra of the secondary electrons were studied using an electron spectrometer equipped with an electrostatic hemispherical analyzer [40]. The DDCSs were measured over the energy range of 1 to 300 eV and for the emission angles between 20° and 150°. The 99% pure C_{60} powder was heated in a metallic oven at approximately 550 °C to obtain an effusive molecular jet target. The fluctuations in the C_{60} vapor yield were monitored in real time using a quartz-crystal-based thickness monitor *in situ*. Similar DDCS spectra were also measured using an atomic target, such as the Ne gas target, in the same experimental run to check the spectrometer performance, particularly in the low-energy part of the spectrum. The Ne target was used under the static gas pressure condition and the absolute cross sections were estimated from the first principle [40]. The SIMION software was used to ensure 100% transmission through the analyzer over the entire electron energy range. The performance of the spectrometer was tested experimentally in order to reproduce the well-known shape of the continuum electron emission spectrum and the binary encounter elastic peak in ion-atom collisions (see Ref. [40] for details). The same spectrometer has been widely used to investigate several features of Coulomb ionization in ion-atom or ion-molecule collisions using He, Ne, H_2, or other heavier atoms and large biomolecules [1,38,40–42]. However, in order to compare the shape of the two spectra arising from Ne and C_{60}, the Ne data was normalized to that for C_{60} at a given energy since the gas density, path length, and solid angles were different for the two cases. The angular efficiency of the spectrometer depends on the solid-angle path-length integral, which is known to vary as $1/\sin\theta$ [40,43] in the case of the static gas target. However, for the jet target C_{60}, we estimated the solid-angle path-length integral, convoluted with the gas density, using the approach given by Scoles *et al.* [44]. The size of the target in the interaction zone was estimated using the aspect ratio for the C_{60} heater nozzle. The angular correction factor deviated from $1/\sin\theta$ dependence at angles other than 90°.

In the present experiment, in order to obtain the absolute DDCS for C_{60}, we employed a self-normalization technique in which the area under the KLL-Auger electron peak in the DDCS spectrum for the C_{60} target was determined and normalized to the absolute carbon KLL-Auger electron cross section. The absolute KLL-Auger electron cross section for carbon was determined using a methane target, under static gas pressure condition, by integrating the DDCS data over the KLL energy range and over all of the angles. This total cross section of KLL-Auger electron emission for the methane target was then used to normalize the total (integrated) KLL-Auger yield for the C_{60} target. We have assumed that the methane and the C_{60} targets have the same cross section (per C atom) for the KLL-Auger electron emission process. More details on the normalization procedure are given in our earlier work [1] and also discussed in the Appendix. The overall uncertainty in the absolute cross-section data was estimated to be ~20–25%, which arises mainly from the target density fluctuations, normalization procedure, peak fitting, and statistics.

III. RESULTS AND DISCUSSIONS

A. Electron energy dependence of DDCS

In Figs. 1(a)–1(d), we have shown the e^- -DDCS (as a function of electron energy $d\epsilon_e$ and solid angle $d\Omega_e$) for the C_{60} and the Ne atom measured at angles 30°, 60°, 90°, and 135°. The peak observed at the energy 230 eV corresponds to the C KLL-Auger electrons, as clearly seen in each plot as well as in the inset of the upper corner in Fig. 1(d). In the case of the Ne target, a continuum spectrum is observed whose shape is typical of that in an ion-atom collision process. The spectral shape [Fig. 1(a)] for C_{60} in a high-energy region ($\geqslant$40 eV) is similar to that for the Ne target, whereas in the low-energy part of the spectrum the shape is remarkably different. It should be

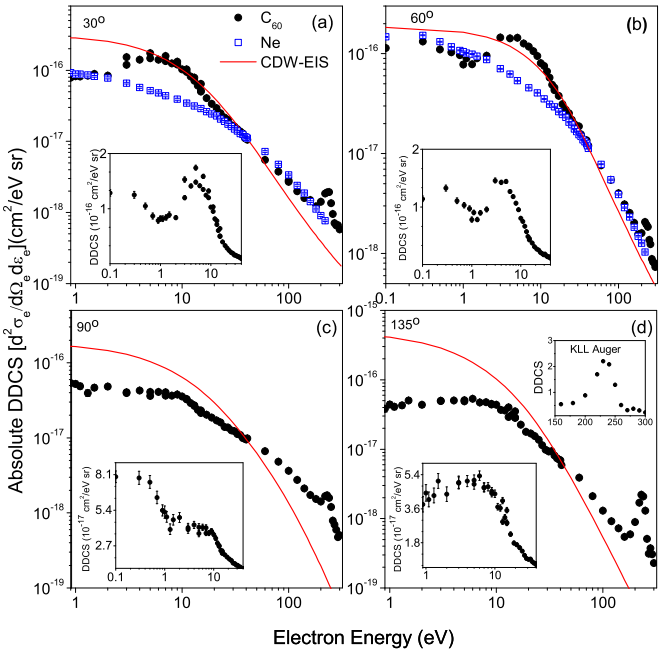

FIG. 1. (Color online) Energy distribution of absolute e^--DDCS for C_{60} (filled symbols), Ne (open symbols), and the CDW-EIS model for the single C atom (solid line). The Ne data and CDW-EIS(C) calculations have been normalized to the C_{60} DDCS at 40 eV. Insets highlight the plasmon-peak region. In (d), the inset in the upper corner shows the KLL peak.

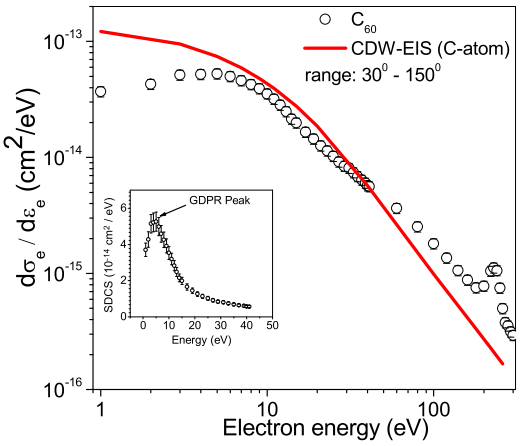

FIG. 2. (Color online) Electron-SDCS spectrum along with the normalized CDW-EIS prediction (red solid line) for a C atom (normalized at one point). Inset: The same electron-SDCS spectrum in linear scale.

mentioned here that the Ne gas target was used at a static pressure and the fullerene was obtained as a vapor target in the form of a jet and hence the path-length solid angle and density will be different for the two cases. Therefore, the absolute data for these two targets cannot be compared. For convenience, we have normalized the Ne data to that for the fullerene at 40 eV in order to compare the shape of the spectrum. One can clearly see a broad hump in the energy range of 1–15 eV, in the spectrum of C_{60}, which is due to the deexcitation of the GDPR state. It is to be noted that unlike in the case of the photoabsorption [4,29] or the electron energy loss spectroscopy (EELS) studies [5,32], in the case of ionization through ion impact, the kinetic energy of the electrons will be reduced by an amount equal to the ionization potential of C_{60}. The first ionization potential of the C_{60} is 7.6 eV (in the vapor phase) [45]. However, there are several states below the highest occupied molecular orbital (HOMO, h_u) up to an energy of ∼12 eV and beyond, in the valence shell [46]. Hence, the GDPR peak is shifted towards the lower-energy side compared to the expected energy of (∼20−7.6) ∼ 12.4 eV obtained by considering only the first ionization potential. The peak position and width of the plasmon resonance will also depend on the shape and angular distribution of the Coulomb-ionization continuum background, which is substantial in this energy range. Therefore, we observe the peak position around 6–9 eV and typical width around 10–12 eV, at different angles, in agreement with an earlier study [4]. For the C_{60} molecule, which is a multiatomic multielectronic system, accurate quantum theoretical treatments are rather difficult. Although excellent theoretical advances have been made in the field of photon and electron collisions with C_{60} [9,32,33,47–49], the theoretical treatment of heavy-ion C_{60} collisions has remained a challenge. Due to this limitation, we have compared the DDCS data with the predictions of an ion-atom collision model, namely, the continuum-distorted-wave eikonal-initial-state (CDW-EIS) model [50–52], for the atomic carbon target. As shown in Figs. 1(a)–1(d), the model prediction (normalized to data in each panel) fails to match the measured spectrum. This is expected since the model does not include many-body effects, the electron correlations, and the collective behavior, which play prominent roles in collisions with the C_{60} molecules.

B. Single-differential distribution

Furthermore, single-differential cross sections (SDCSs) in energy are shown in Fig. 2 along with the CDW-EIS calculations. The GDPR peak is also clearly visible in the energy SDCS spectrum plotted. The agreement with the CDW-EIS model improves slightly in the high-energy region. In fact, upon careful inspection of the SDCS spectrum, one can also see a slight slope change near 30 eV electron energy. This is remarkably close to the expected energy range for second plasmon excitation [29]. Furthermore, a better agreement between experiment and the CDW-EIS model (in the high-energy region) for SDCS as compared to DDCS reaffirms the need for an *ab initio* model to describe the dynamics of a heavy-ion C_{60} collision at the DDCS level. From the SDCS spectrum, we have also estimated the fractional contribution of GDPR electrons to the total cross section to be nearly 50%, which is in close agreement with that estimated earlier [26,28] for different projectiles.

C. Angular distributions

The angular distribution of the plasmon electrons gives information regarding the nature of collective oscillation, i.e., whether it is dipole- or quadrupole-type resonance. In Figs. 3(a)–3(d), we present the angular distribution of the

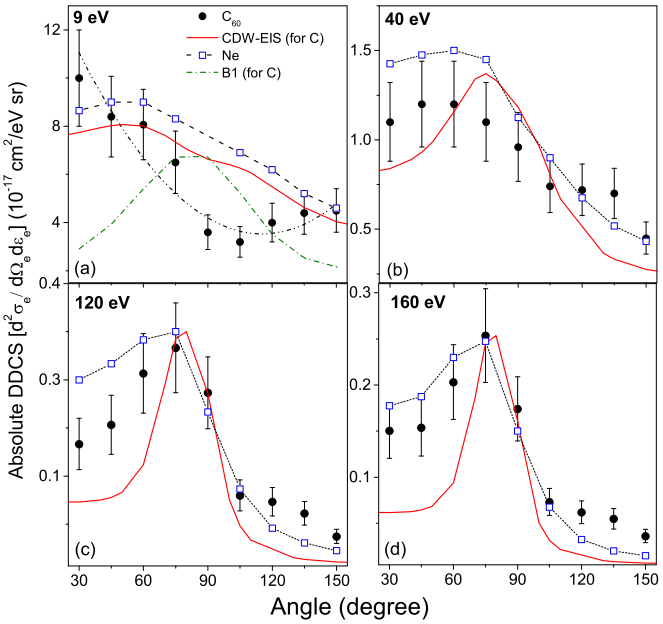

FIG. 3. (Color online) Angular distribution of e^--DDCS for C_{60} (filled circles) and Ne (open squares joined by dotted line). The CDW-EIS (solid line) and the B1 (dash-dotted line) calculations for the C atom are also shown. The data for the Ne and the CDW-EIS calculations are normalized to the C_{60} data in each plot. The dash-double-dotted line through the C_{60} data points for 9 eV electrons in (a) is to guide the eyes.

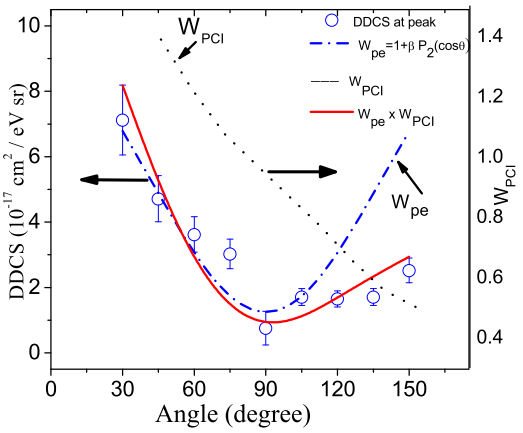

FIG. 4. (Color online) Measured e^--DDCS for C_{60} (circles) target, same as in Fig. 2(a), along with the calculated distributions: W_{pe} (dash-dotted line), W_{PCI} (dotted line: scale on right axis), and total distribution $W_{\rm tot}$ (thick solid line).

electron-DDCS for the C_{60} target for four different emission energies, i.e., 9, 40, 120, and 160 eV, in the angular range of 30° to 150°. For electrons at the GDPR peak [i.e., ∼9 eV: "plasmon electrons" in Fig. 3(a)], the angular distribution shows a dip at 90° and the electron emission is predominantly in the forward and backward direction with respect to the projectile beam momentum vector. This is in sharp contrast to the distribution observed in usual ion-atom collision experiments as also evident from the Ne data and the CDW-EIS calculation for the C atom plotted in the same graph. Such distribution can be explained in terms of a soft collision, two-center effect, or a binary collision mechanism, which are included in the CDW-EIS model for direct ionization of an electron by the fast ions. In the case of the fullerene, the electron emission at the plasmon peak, i.e., around 9 eV, is dominated by the decay of plasmon which is excited by the swift ions. The long-range Coulomb interaction of the projectile ions at a large distance and the restoring force of the positive core drives the oscillation. A primarily forward-backward emission of electrons, in our case, suggests a preferential excitation of the plasmon oscillations along the projectile beam direction. In the present collision system, the projectile dwell time (just to cross the molecular electron cloud) is 1.6 a.u. ($\sim 3.5 \times 10^{-17}$ sec ($v_p \sim 13$ a.u.), which is about five times faster than the period of plasmon oscillation (i.e., ∼8 a.u., $\sim 1.8 \times 10^{-16}$ sec) in C_{60}. Due to the long-range Coulomb interaction, the electron cloud feels a sudden impulse before the projectile actually crosses the molecule, causing a displacement of the electron cloud which gives rise to an induced dipole moment of the collective state along the projectile beam direction. This combined with the restoring force due to the positive-ion core causes an oscillation of the cloud along the ion-beam axis and prevails even after the collision. Therefore, the angular distribution of the electron emission will correspond to that due to an oscillating dipole aligned approximately along the ion-beam axis.

The observed angular distribution data is well reproduced (dash-dotted line in Fig. 4) for most of the forward angles by the photoelectron angular distribution for linearly polarized light which is given by [36,53] $W_{pe}(\theta) \sim \{1 + \beta P_2[\cos(\theta - \theta_0)]\}$, with θ being the angle of electron emission with respect to the polarization axis and θ_0 being the angle of polarization measured relative to the ion-beam axis. Based on the above discussion, we may choose $\theta_0 \sim 0$. The model predicts a nearly symmetric distribution around 90°, whereas the data show an asymmetric distribution. The forward-backward asymmetry is caused due to the postcollisional interaction (PCI) [54] of the emitted electron with the projectile ions. In PCI, the distortion of the electron wave function in the final state due to the influence of the two moving Coulomb centers (target ion and projectile ion) is considered. This gives rise to a forward focusing of electrons and a backward depletion [55–58]. Such a PCI is well described by the CDW-EIS model [51] (and references therein). The contribution due to the PCI is expected to be substantial since the Coulomb perturbation strength $q/v_p \sim 0.7$ is reasonably strong. To estimate the amount of asymmetry caused due to the PCI, we get help from the B1 (first Born) approximation. The B1, which is a single-center (target center in this case) model, does not include any PCI and hence predicts an almost symmetric angular distribution [see dash-dotted line in Fig. 2(a)]. The ratio of the CDW-EIS prediction to that of the B1 calculation, i.e., DDCS(CDW-EIS)/DDCS(B1), then gives a reasonable estimate of the correction factor $W_{PCI}(\theta)$ due to the PCI (dotted line in Fig. 4). The total distribution is therefore given by $W_{\rm tot} = N[1 + \beta P_2(\cos\theta)]W_{PCI}$ (solid line in Fig. 4), which is in excellent agreement with the observed angular distribution of the electron DDCS at the plasmon peak. The final distribution $W_{\rm tot}$ was obtained using the anisotropy parameter $\beta = 1.4$ and a normalization constant (N), in order to match the distribution with the experimental DDCS at a

given forward angle. However, a slightly different choice for the values of β and θ_0 cannot be ruled out.

Further, at higher electron energies [Figs. 3(b)–3(d)], the angular distribution for C_{60} gradually shows similar behavior as that for the Ne target with the DDCS peaking close to 90°. The qualitative agreement between the CDW-EIS (for C atom) and the data for C_{60} also improves. This signifies the dominance of the low-impact parameter binary collisions of ions with individual C atoms in the molecule, whereas, as shown above, the low-energy electrons carry the signature of the molecular nature of the target and hence of the plasmon excitation. The GDPR peak retains its signature in the SDCS (single-differential cross sections, $d\sigma/d\epsilon_e$) spectrum, derived after integration of the DDCS over θ.

As shown above, the collective excitation peak corresponds to almost 50% of the total ionization process; this may also imply that the collective excitation and similar many-body effects which are responsible for a large amount of electron emission at low energy must be considered for modeling any practical application, such as heavy-ion-induced radiation damage of the biological cells or DNA bases, or nanoparticles [39]. The decay of collective plasmon excitations in fullerene thus provides a mechanism to enhance the low-energy electrons which is consistent with that predicted, very recently, in other carbon-based nanosystems [39].

IV. CONCLUSIONS

We have presented a detailed measurement of the energy and angular distribution of the DDCS of low-energy electrons emitted from a C_{60} fullerene molecule in collisions with fast bare F ions of energy 4 MeV/u. The normalization procedure employs a different technique which uses the absolute cross section of carbon KLL-Auger electron emission measured *in situ* using a CH_4 target. The dominant role of the GDPR on the electron-DDCS spectrum from a free C_{60} molecule has been explored in which a fast heavy ion has been used as a probe. A clear manifestation of the characteristic "plasmon-electron" peak has been emphasized. It is estimated that the plasmon excitation mechanism alone contributes a large fraction, i.e., about 50%, of the total electron emission in such collisions. The angular distribution of the plasmon electrons shows a dip in the transverse direction which is dramatically different from the observed behavior for an atomic target, measured *in situ*, as well as the predictions of quantum mechanical models for ion-atom collisions. A simple model, based on the concept of photoelectron distribution applied to a linearly polarized dipole oscillating along the ion-beam axis, combined with the postcollisional interaction, is shown to reproduce the plasmon-electron angular distribution in an excellent manner. However, for the higher-energy electron emission, the angular distribution shows a peak which is similar to that observed in ion-atom collisions. The derived single-differential spectrum also reveals the broad plasmon-electron peak.

ACKNOWLEDGMENTS

The authors would like to thank the Pelletron staff at TIFR, Mumbai, for smooth operation of the accelerator during the experiments. We would also like to thank Deepankar Misra and Siddharth Kasthurirangan for their help during the experiment and for many discussions. We are also grateful to Eric Suraud for valuable input.

APPENDIX: NORMALIZATION PROCEDURE

In the case of a collision with an effusive jet, it is difficult to estimate absolute DDCS based on the first principle since the jet geometry, the degree of overlap with the ion beams, and the solid-angle path-length integral are not known exactly. The absolute normalization of the electron DDCS data was thus done with the help of the carbon KLL-Auger intensity. In the first step, the experiment was carried out with a methane gas under static pressure condition, using the same scattering chamber and same spectrometer. The absolute values for DDCSs for a CH_4 gas target were obtained from the first principle [40], i.e., by knowing the quantities such as the beam intensity, target thickness, solid-angle path-length integral, dimensions of the apertures, and resolution of the spectrometer. The target thickness was deduced from the pressure determined by a well-calibrated MKS Baratron pressure gauge. The front of the channel electron multiplier (CEM) was raised to a voltage of 100 volts. Therefore, effectively all of the low-energy electrons up to 500 eV were detected with same efficiency since the efficiency of the CEM in this energy range, i.e., 100–500 eV, is constant, which is about 0.83 as obtained from the manual of the CEM. The background spectrum was collected with no gas in the chamber. The absolute DDCS spectrum for the CH_4 target was then deduced after background subtraction. The integration of this spectrum over the carbon KLL-Auger peak region for each angle provides the single-differential cross section (SDCS $= \frac{d\sigma}{d\Omega}$) for the KLL-Auger process. After integrating the SDCS (KLL) over all measured angles, the absolute total carbon KLL-Auger emission cross section (σ_{KLL}) was then obtained.

In the second step, the experiment was conducted with the effusive jet target of fullerene. The relative DDCS were measured for different angles and then the relative SDCS was derived. The relative SDCS ($\frac{d\sigma}{dE}$) spectrum for the ionization of fullerene was plotted (Fig. 2). This spectrum which was obtained from the jet target has two parts: (1) the low-energy continuum part and (2) the carbon KLL-Auger peak at around 230 eV. Both parts of the spectrum are thus produced from the same target thickness, jet profile, beam overlap with jet, and are associated with the same solid angle. Then by integrating the SDCS ($\frac{d\sigma}{dE}$) spectrum over the electron energy across the C KLL-Auger line, the yield (Y_{KLL}) of the KLL-Auger process was then obtained. The yield is given by $Y_{KLL} = \sigma_{KLL} S \epsilon(E) N_p$, where S represents the target thickness convoluted with the jet profile and path-length integral. The number of projectile ions is denoted by N_p. Here we have assumed that the carbon KLL-Auger emission cross section (σ_{KLL}) is the same as in the case of fullerene and the CH_4 molecule, since it arises from a vacancy created in the inner shell, i.e., strongly bound K shell here. However, this assumption also introduces an error. In this way, the unknown quantity S was determined which was then used to normalize the entire electron DDCS spectrum (i.e., 1 and 2) obtained for the C_{60} target. The error estimated in the normalization procedure is ∼20–25%.

[1] A. N. Agnihotri, S. Nandi, S. Kasthurirangan, A. Kumar, M. E. Galassi, R. D. Rivarola, C. Champion, and L. C. Tribedi, Doubly differential distribution of electron emission in ionization of uracil in collisions with 3.5-MeV/u bare C ions, Phys. Rev. A **87**, 032716 (2013).

[2] Y. Ling and C. Lifshitz, Plasmon excitation in polycyclic aromatic hydrocarbons studied by photoionization, Chem. Phys. Lett. **257**, 587 (1996).

[3] G. F. Bertsch, A. Bulgac, D. Tománek, and Y. Wang, Collective Plasmon Excitations in C_{60} Clusters, Phys. Rev. Lett. **67**, 2690 (1991).

[4] I. V. Hertel, H. Steger, J. de Vries, B. Weisser, C. Menzel, B. Kamke, and W. Kamke, Giant Plasmon Excitation in Free C_{60} and C_{70} Molecules Studied by Photoionization, Phys. Rev. Lett. **68**, 784 (1992).

[5] T. Pichler, M. Knupfer, M. S. Golden, J. Fink, and T. Cabioćh, Electronic structure and optical properties of concentric-shell fullerenes from electron-energy-loss spectroscopy in transmission, Phys. Rev. B **63**, 155415 (2001).

[6] S. Hunsche, T. Starczewski, A. l'Huillier, A. Persson, C.-G. Wahlström, H. B. van Linden van den Heuvell, and S. Svanberg, Ionization and Fragmentation of C_{60} via Multiphoton-Multiplasmon Excitation, Phys. Rev. Lett. **77**, 1966 (1996).

[7] S. W. J. Scully, E. D. Emmons, M. F. Gharaibeh, R. A. Phaneuf, A. L. D. Kilcoyne, A. S. Schlachter, S. Schippers, A. Müller, H. S. Chakraborty, M. E. Madjet, and J. M. Rost, Photoexcitation of a Volume Plasmon in C_{60} Ions, Phys. Rev. Lett. **98**, 179602 (2007).

[8] A. V. Korol and A. V. Solov'yov, Comment on Photoexcitation of a Volume Plasmon in C_{60} Ions, Phys. Rev. Lett. **98**, 179601 (2007).

[9] P. Bolognesi, L. Avaldi, A. Ruocco, A. Verkhovtsev, A. V. Korol, and A. V. Solov'yov, Collective excitations in the electron energy loss spectra of C_{60}, Eur. Phys. J. D **66**, 254 (2012).

[10] J.-P. Connerade and A. V. Solov'yov, Giant resonances in photon emission spectra of metal clusters, J. Phys. B: At. Mol. Opt. Phys. **29**, 3529 (1996).

[11] J. P. Connerade, A. G. Lyalin, R. Semaoune, S. K. Semenov, and A. V. Solov'yov, A simple atomic model for hydrogen confined inside a prolate-shaped C_{60} fullerene cage, J. Phys. B: At. Mol. Opt. Phys. **34**, 2505 (2001).

[12] A. V. Korol and A. V. Solov'yov, Polarizational bremsstrahlung of electrons in collisions with atoms and clusters, J. Phys. B: At. Mol. Opt. Phys. **30**, 1105 (1997).

[13] L. G. Gerchikov, A. V. Solov'yov, J.-P. Connerade, and W. Greiner, J. Phys. B: At. Mol. Opt. Phys. **30**, 4133 (1997).

[14] J. P. Connerade and A. V. Solov'yov, Formalism for multiphoton plasmon excitation in jellium clusters, Phys. Rev. A **66**, 013207 (2002).

[15] K. A. Brueckner and R. Thieberger, Nuclear Giant Dipole Resonance, Phys. Rev. Lett. **4**, 466 (1960).

[16] F. Calvayrac, P. G. Reinhard, E. Suraud, and C. A. Ullrich, Nonlinear electron dynamics in metal clusters, Phys. Rep. **337**, 493 (2000).

[17] D. L. Ederer, Photoionization of the 4d Electrons in Xenon, Phys. Rev. Lett. **13**, 760 (1964).

[18] J. Burgdörfer, Dynamic screening and wake effects on electronic excitation in ion-solid and ion-surface collisions, Nucl. Instrum. Methods Phys. Res. B **67**, 1 (1992).

[19] P. M. Echenique, R. H. Ritchie, and W. Brandt, Spatial excitation patterns induced by swift ions in condensed matter, Phys. Rev. B **20**, 2567 (1979).

[20] L. C. Tribedi, V. Nanal, M. R. Press, M. B. Kurup, K. G. Prasad, and P. N. Tandon, Radiative electron capture by fully stripped channeled light ions, Phys. Rev. A **49**, 374 (1994).

[21] L. C. Tribedi, V. Nanal, M. B. Kurup, K. G. Prasad, and P. N. Tandon, Radiative electron capture by bare and H-like Si and Cl ions using the channeling technique and the associated solid-state effect, Phys. Rev. A **51**, 1312 (1995).

[22] J. M. Pitarke, R. H. Ritchie, and P. M. Echenique, Radiative electron capture by channeled ions, Phys. Rev. B **43**, 62 (1991).

[23] S. Datz, C. D. Moak, O. H. Crawford, H. F. Krause, P. F. Dittner, J. Gomez del Campo, J. A. Biggerstaff, P. D. Miller, P. Hvelplund, and H. Knudsen, Resonant Coherent Excitation of Channeled Ions, Phys. Rev. Lett. **40**, 843 (1978).

[24] T. Azuma, T. Ito, K. Komaki, Y. Yamazaki, M. Sano, M. Torikoshi, A. Kitagawa, E. Takada, and T. Murakami, Impact Parameter Dependent Resonant Coherent Excitation of Relativistic Heavy Ions Planar Channeled in Crystals, Phys. Rev. Lett. **83**, 528 (1999).

[25] U. Kadhane, D. Misra, Y. P. Singh, and L. C. Tribedi, Effect of Collective Response on Electron Capture and Excitation in Collisions of Highly Charged Ions with Fullerenes, Phys. Rev. Lett. **90**, 093401 (2003).

[26] T. LeBrun, H. G. Berry, S. Cheng, R. W. Dunford, H. Esbensen, D. S. Gemmell, E. P. Kanter, and W. Bauer, Ionization and multifragmentation of C_{60} by High-Energy, Highly Charged Xe Ions, Phys. Rev. Lett. **72**, 3965 (1994).

[27] S. Cheng, H. G. Berry, R. W. Dunford, H. Esbensen, D. S. Gemmell, E. P. Kanter, T. LeBrun, and W. Bauer, Ionization and fragmentation of C_{60} by highly charged, high-energy xenon ions, Phys. Rev. A **54**, 3182 (1996).

[28] H. Tsuchida, A. Itoh, Y. Nakai, K. Miyabe, and N. Imanishi, Cross sections for ionization and fragmentation of C_{60} by fast H^+ impact, J. Phys. B: At. Mol. Opt. Phys. **31**, 5383 (1998).

[29] S. W. J. Scully, E. D. Emmons, M. F. Gharaibeh, R. A. Phaneuf, A. L. D. Kilcoyne, A. S. Schlachter, S. Schippers, A. Müller, H. S. Chakraborty, M. E. Madjet, and J. M. Rost, Photoexcitation of a Volume Plasmon in C_{60} Ions, Phys. Rev. Lett. **94**, 065503 (2005).

[30] U. Kadhane, A. Kelkar, D. Misra, A. Kumar, and L. C. Tribedi, Effect of giant plasmon excitations in single and double ionization of C_{60} in fast heavy-ion collisions, Phys. Rev. A **75**, 041201(R) (2007).

[31] A. H. Kelkar, U. Kadhane, D. Misra, L. Gulyás, and L. C. Tribedi, Single and multiple ionization of C_{60} fullerenes and collective effects in collisions with highly charged C, F, and Si ions with energy 3 MeV/u, Phys. Rev. A **82**, 043201 (2010).

[32] A. V. Verkhovtsev, A. V. Korol, A. V. Solov'yov, P. Bolognesi, A. Ruocco, and L. Avaldi, Interplay of the volume and surface plasmons in the electron energy loss spectra of C_{60}, J. Phys. B: At. Mol. Opt. Phys. **45**, 141002 (2012).

[33] A. V. Solov'yov, Plasmon excitations in metal clusters and fullerenes, Int. J. Mod. Phys. B **19**, 4143 (2005).

[34] J. M. Keller and M. A. Coplan, Electron energy los spectroscopy of C_{60}, Chem. Phys. Lett. **193**, 89 (1992).

[35] B. D. DePaola, R. Parameswaran, B. P. Walch, M. D. Troike, P. Richard, M. J. Puska, and R. M. Nieminen, Experimental

determination of the compton profile of C_{60} through binary encounter electron spectroscopy, J. Chem. Phys. **103**, 10413 (1995).

[36] J. O. Johansson, G. G. Henderson, F. Remacle, and E. E. B. Campbell, Angular-Resolved Photoelectron Spectroscopy of Superatom Orbitals of Fullerenes, Phys. Rev. Lett. **108**, 173401 (2012).

[37] A. Verkhovtsev, S. McKinnon, P. de Vera, E. Surdutovich, S. Guatelli, A. V. Korol, A. Rosenfeld, and A. V. Solov'yov, Comparative analysis of the secondary electron yield from carbon nanoparticles and pure water medium, Eur. Phys. J. D. **69**, 116 (2015).

[38] N. Stolterfoht, B. Sulik, V. Hoffmann, B. Skogvall, J. Y. Chesnel, J. Rangama, F. Frémont, D. Hennecart, A. Cassimi, X. Husson, A. L. Landers, J. A. Tanis, M. E. Galassi, and R. D. Rivarola, Evidence for Interference Effects in Electron Emission from H_2 Colliding with 60 MeV/u Kr^{34+} Ions, Phys. Rev. Lett. **87**, 023201 (2001).

[39] D. Misra, U. Kadhane, Y. P. Singh, L. C. Tribedi, P. D. Fainstein, and P. Richard, Interference Effect in Electron Emission in Heavy Ion Collisions with H_2 Detected by Comparison with the Measured Electron Spectrum from Atomic Hydrogen, Phys. Rev. Lett. **92**, 153201 (2004).

[40] D. Misra, K. V. Thulasiram, W. Fernandes, A. H. Kelkar, U. Kadhane, A. Kumar, Y. P. Singh, L. Gulyás, and L. C. Tribedi, Double differential distributions of electron emission in ion-atom and electron-atom collisions using an electron spectrometer, Nucl. Instrum. Methods Phys. Res. B **267**, 157 (2009).

[41] D. Misra, A. Kelkar, U. Kadhane, A. Kumar, Y. P. Singh, L. C. Tribedi, and P. D. Fainstein, Angular distribution of low-energy electron emission in collisions of 6-MeV/u bare carbon ions with molecular hydrogen: Two-center mechanism and interference effect, Phys. Rev. A **75**, 052712 (2007).

[42] Shubhadeep Biswas, J. M. Monti, C. A. Tachino, R. D. Rivarola, and L. C. Tribedi, Differential electron emission in the ionization of Ne and Xe atoms under fast bare carbon ion impact, J. Phys. B: At. Mol. Opt. Phys. **48**, 115206 (2015).

[43] M. W. Gealy, G. W. Kerby, Y. Y. Hsu, and M. E. Rudd, Energy and angular distributions of electrons from ion impact on atomic and molecular hydrogen. I. 20–114-keV $H^+ + H_2$, Phys. Rev. A **51**, 2247 (1995).

[44] G. Scoles, *Atomic and Molecular Beam Methods* (Oxford University Press, New York, 1988).

[45] J. de Vries, H. Steger, B. Kamke, C. Menzel, B. Weisser, W. Kamke, and I. Hertel, Single-photon ionization of C_{60}- and C_{70}-fullerene with synchrotron radiation: Determination of the ionization potential of C_{60}, Chem. Phys. Lett. **188**, 159 (1992).

[46] D. L. Lichtenberger, K. W. Nebesny, C. D. Ray, D. R. Huffman, and L. D. Lamb, Valence and core photoelectron spectroscopy of C_{60}, buckminsterfullerene, Chem. Phys. Lett. **176**, 203 (1991).

[47] V. K. Ivanov, G. Y. Kashenock, R. G. Polozkov, and A. V. Solov'yov, J. Phys. B: At. Mol. Opt. Phys. **34**, L669 (2001).

[48] M. E. Madjet, H. S. Chakraborty, J. M. Rost, and S. T. Manson, Photoionization of C_{60}: A model study, J. Phys. B: At. Mol. Opt. Phys. **41**, 105101 (2008).

[49] A. Verkhovtsev, A. V. Korol, and A. V. Solov'yov, Formalism of collective electron excitations in fullerenes, Eur. Phys. J. D. **66**, 253 (2012).

[50] D. S. F. Crothers and J. F. McCann, Ionisation of atoms by ion impact, J. Phys. B: At. Mol. Opt. Phys. **16**, 3229 (1983).

[51] P. D. Fainstein, V. H. Ponce, and R. D. Rivarola, Two-centre effects in ionization by ion impact, J. Phys. B: At. Mol. Opt. Phys. **24**, 3091 (1991).

[52] L. Gulyás, P. Fainstein, and A. Salin, CDW-EIS theory of ionization by ion impact with Hartree-Fock description of the target, J. Phys. B: At. Mol. Opt. Phys. **28**, 245 (1995).

[53] J. Cooper and R. N. Zare, Angular distribution of photoelectrons, J. Chem. Phys. **48**, 942 (1968).

[54] M. U. Kuchiev and S. A. Sheĭnerman, Post-collision interaction in atomic processes, Sov. Phys. Usp. **32**, 569 (1989).

[55] N. Stolterfoht, H. Platten, G. Schiwietz, D. Schneider, L. Gulyás, P. D. Fainstein, and A. Salin, Two-center electron emission in collisions of fast, highly charged ions with he: Experiment and theory, Phys. Rev. A **52**, 3796 (1995).

[56] R. Moshammer, J. Ullrich, M. Unverzagt, W. Schmidt, P. Jardin, R. E. Olson, R. Mann, R. Dörner, V. Mergel, U. Buck, and H. Schmidt-Böcking, Low-Energy Electrons and Their Dynamical Correlation with Recoil Ions for Single Ionization of Helium by Fast, Heavy-Ion Impact, Phys. Rev. Lett. **73**, 3371 (1994).

[57] M. Schulz, R. Moshammer, D. Fischer, H. Kollmus, D. Madison, S. Jones, and J. Ullrich, Three-dimensional imaging of atomic four-body processes, Nature (London) **422**, 48 (2003).

[58] N. V. Maydanyuk, A. Hasan, M. Foster, B. Tooke, E. Nanni, D. H. Madison, and M. Schulz, Fully Differential Studies on Single Ionization of Helium by Slow Proton Impact, Phys. Rev. Lett. **94**, 243201 (2005).